nature cell biology

Toll-like receptor activation suppresses ER stress factor CHOP and translation inhibition through activation of eIF2B

Connie W. Woo[1], Lydia Kutzler[2], Scot R. Kimball[2] and Ira Tabas[1,3]

Activation of Toll-like receptors (TLRs) induces the endoplasmic reticulum (ER) unfolded protein response (UPR) to accommodate essential protein translation[1,2]. However, despite increased levels of phosphorylated eIF2α (p-eIF2α), a TLR–TRIF-dependent pathway assures that the cells avoid CHOP induction, apoptosis and translational suppression of critical proteins[3]. As p-eIF2α decreases the functional interaction of eIF2 with eIF2B, a guanine nucleotide exchange factor (GEF), we explored the hypothesis that TLR–TRIF signalling activates eIF2B GEF activity to counteract the effects of p-eIF2α. We now show that TLR–TRIF signalling activates eIF2B GEF through PP2A-mediated serine dephosphorylation of the eIF2B ε-subunit. PP2A itself is activated by decreased Src-family-kinase-induced tyrosine phosphorylation of its catalytic subunit. Each of these processes is required for TLR–TRIF-mediated CHOP suppression in ER-stressed cells *in vitro* and *in vivo*. Thus, in the setting of prolonged, physiologic ER stress, a unique TLR–TRIF-dependent translational control pathway enables cells to carry out essential protein synthesis and avoid CHOP-induced apoptosis while still benefiting from the protective arms of the UPR.

In cells undergoing ER stress, PERK phosphorylates the eukaryotic initiation factor (eIF) 2α (p-eIF2α), which decreases recycling of the essential ternary complex of eIF2, GTP, and initiator methionyl transfer RNA (ref. 4) and thereby decreases the translation initiation of most cellular messenger RNAs (ref. 2). This action also enhances the translation of the mRNA encoding ATF4, which then induces CEBP-homologous protein[2] (CHOP, also known as DDIT3 and GADD153). During physiologic ER stress, transient CHOP expression is beneficial, but in pathologically chronic ER stress, prolonged CHOP expression promotes cell death and has been implicated in a number of diseases, including neurodegenerative diseases, atherosclerosis, diabetes and renal disease[5,6]. It therefore follows that in cells that require a physiologic uninterrupted UPR response, prolonged expression of CHOP and suppression of global protein synthesis would have to be at least partially abrogated. In the case of macrophages exposed to activators of TLR4 or TLR3, this function is effected by a pathway downstream of the adaptor TRIF (also known as TICAM1) that suppresses ATF4 translation and subsequent CHOP induction and maintains global translation in the presence of normal PERK activation and eIF2α phosphorylation[3]. When this pathway is blocked in mice, ER-stress-induced CHOP induction, cell death and organ dysfunction ensue[3].

The goal of this study was to elucidate the molecular signalling components of this adaptive pathway. The above findings indicated that the pathway somehow renders the cells 'resistant' to p-eIF2α, which functions by tightly binding an essential ternary complex GTP-exchange factor (GEF) called eIF2B in a manner that competitively inhibits GDP–GTP exchange on the γ-subunit of eIF2 (ref. 7). In this context, we explored the hypothesis that TLR–TRIF increases the level of eIF2B GEF activity, which might enable adequate GDP–GTP exchange, in the presence of p-eIF2α.

We first determined whether TLR–TRIF signalling increases the level of eIF2B GEF activity in ER-stressed cells. Macrophages from wild-type and *Trif*$^{-/-}$ mice were treated with the ER stressor tunicamycin alone or after pre-treatment of the cells with the TLR4 activator lipopolysaccharide (LPS). As expected from the increase in the level of p-eIF2α in ER-stressed cells[4], tunicamycin suppressed eIF2B GEF activity in both wild-type and *Trif*$^{-/-}$ macrophages (Fig. 1a). However, in LPS-treated wild-type but not *Trif*$^{-/-}$ ER-stressed macrophages, the level of eIF2B GEF activity was increased to that of the control. Thus, TLR–TRIF signalling restores ER-stress-suppressed eIF2B GEF activity to the non-ER-stress level.

One mechanism of eIF2B GEF activation is through dephosphorylation of a pSer residue (termed Ser^{GSK} after the kinase that can phosphorylate it[8]) in the ε-subunit of eIF2B (refs 8,9). LPS pre-treatment partially decreased the pSer^{GSK}-eIF2Bε in both tunicamycin-treated cells and in untreated wild-type but not *Trif*$^{-/-}$ cells (Fig. 1b,c). Thus,

[1]Departments of Medicine, Pathology & Cell Biology, and Physiology & Cellular Biophysics, Columbia University, New York 10032, USA. [2]Department of Cellular and Molecular Physiology, The Pennsylvania State University College of Medicine, Hershey, Pennsylvania 17033, USA.
[3]Correspondence should be addressed to I.T. (e-mail: iat1@columbia.edu)

Received 12 October 2011; accepted 23 November 2011; published online 8 January 2012; DOI: 10.1038/ncb2408

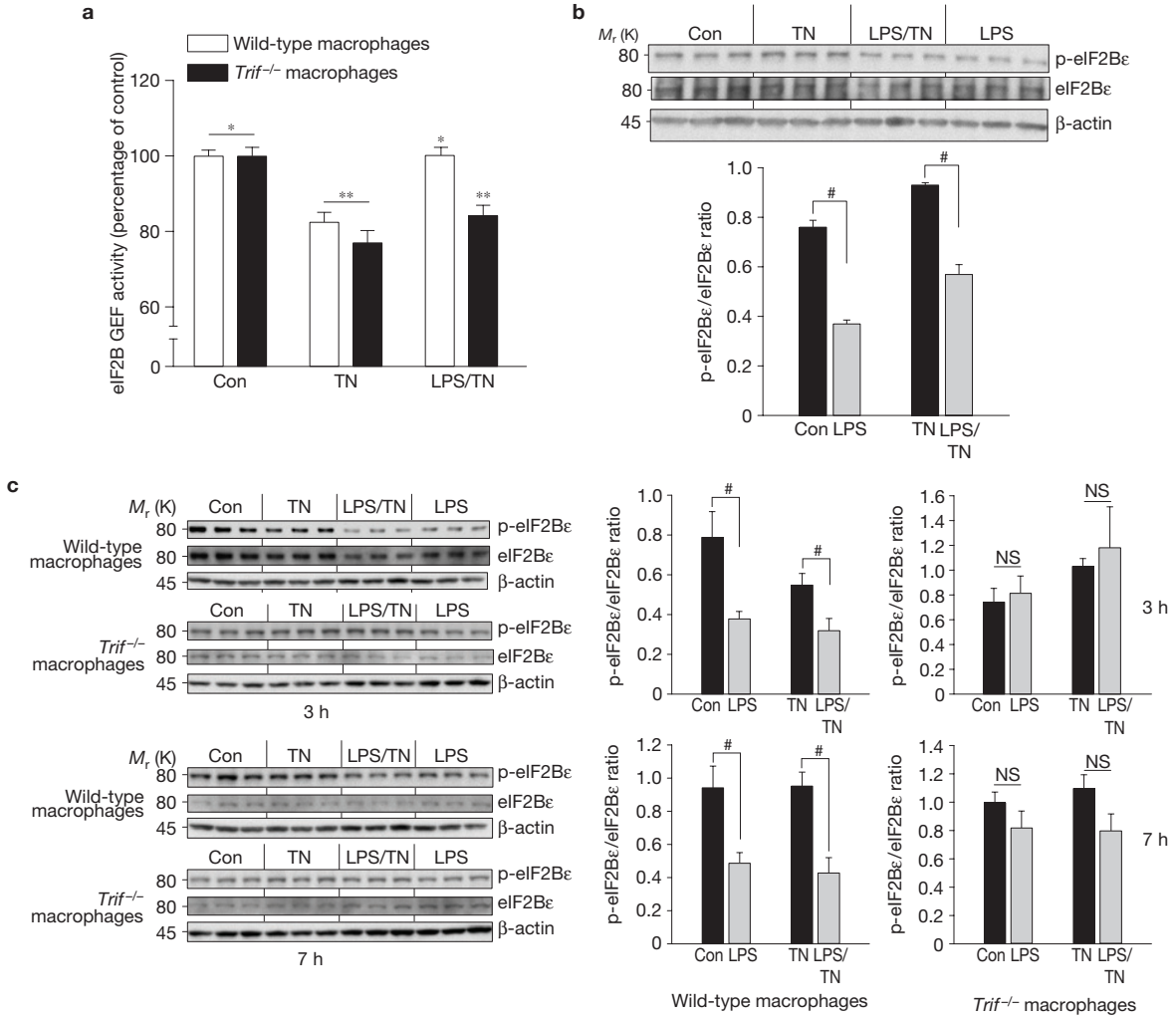

Figure 1 LPS increases guanine nucleotide exchange activity of eIF2B. (**a**) Macrophages from wild-type or *Trif*$^{-/-}$ mice were untreated (Con) or pre-treated (or not) with LPS (1 ng ml^{-1}) for 24 h followed by a 3 h treatment with tunicamycin (TN, 1 μg ml^{-1}). eIF2B GEF activity was then assayed. Data are expressed as mean ± s.e.m. with $n = 6$; bars with different symbols are statistically different from each other, $P \leq 0.02$. (**b**) Cells were treated similarly to those in **a**, except an LPS-alone group was included, and then extracts were analysed by immunoblot analysis (top) for p–eIF2Bε and total eIF2Bε and β-actin as a loading control. Densitometric quantification of the immunoblot data is shown in the histogram as mean ± s.e.m. with $n = 3$. #, $P < 0.05$. (**c**) The same as in **b**, except macrophages from wild-type and *Trif*$^{-/-}$ mice were compared, and data for 7 h of tunicamycin treatment are also shown. #, $P < 0.05$; NS, not significant. Uncropped images of blots are shown in Supplementary Fig. S6.

TRIF is required for the ability of LPS to both increase the level of eIF2B GEF activity and to decrease the level of eIF2B phosphorylation.

The hypothesis predicts that the need for LPS to suppress CHOP could be bypassed by increasing the level of eIF2B GEF activity by an LPS-independent means. We investigated this idea by transfecting murine embryonic fibroblasts (MEFs) with wild-type or S–A^{GSK}-mutant rat *Eif2be* (ref. 10), which should be particularly potent because it cannot be deactivated by phosphorylation (S. Kimball, unpublished data). We first showed that LPS suppresses p-eIF2Bε, CHOP and CHOP-promoter-driven green fluorescent protein (GFP) reporter expression in ER-stressed MEFs (Supplementary Fig. S1a,b), and CHOP suppression was not affected by the transfection reagent, Lipofectamine (Fig. 2a, groups 1–5). Transfection with S–A^{GSK} *Eif2be*, which resulted in a level of total *Eif2be* mRNA (wild-type + mutant) that was approximately twice the endogenous level (Fig. 2a, right), mimicked the effect of LPS in terms of suppressing CHOP expression (Fig. 2a, group 6). Transfection with wild-type *Eif2be* also resulted in CHOP suppression (Fig. 2a, group 7), but the level of suppression was less than that seen with S–A^{GSK} *Eif2be*. Thus, increasing eIF2Bε in ER-stressed MEFs, especially when the ε subunit cannot be phosphorylated, mimics the effect of LPS on CHOP suppression.

We then conducted a series of experiments in which we first silenced endogenous eIF2Bε using a short interfering RNA (siRNA) that targets mouse but not human (h) *EIF2BE*, followed by transfection of these cells with one of various h*EIF2BE* constructs. The siRNA effectively silenced endogenous eIF2Bε, and the decrease in the level of eIF2Bε was associated with a decrease in LPS-induced CHOP suppression (Fig. 2b, upper left). This finding is consistent with the model, because there would be very little GEF to be activated by the eIF2Bε dephosphorylation pathway.

We next transfected the silenced cells with a construct encoding human eIF2Bε with serine–alanine point mutations in both the GSK

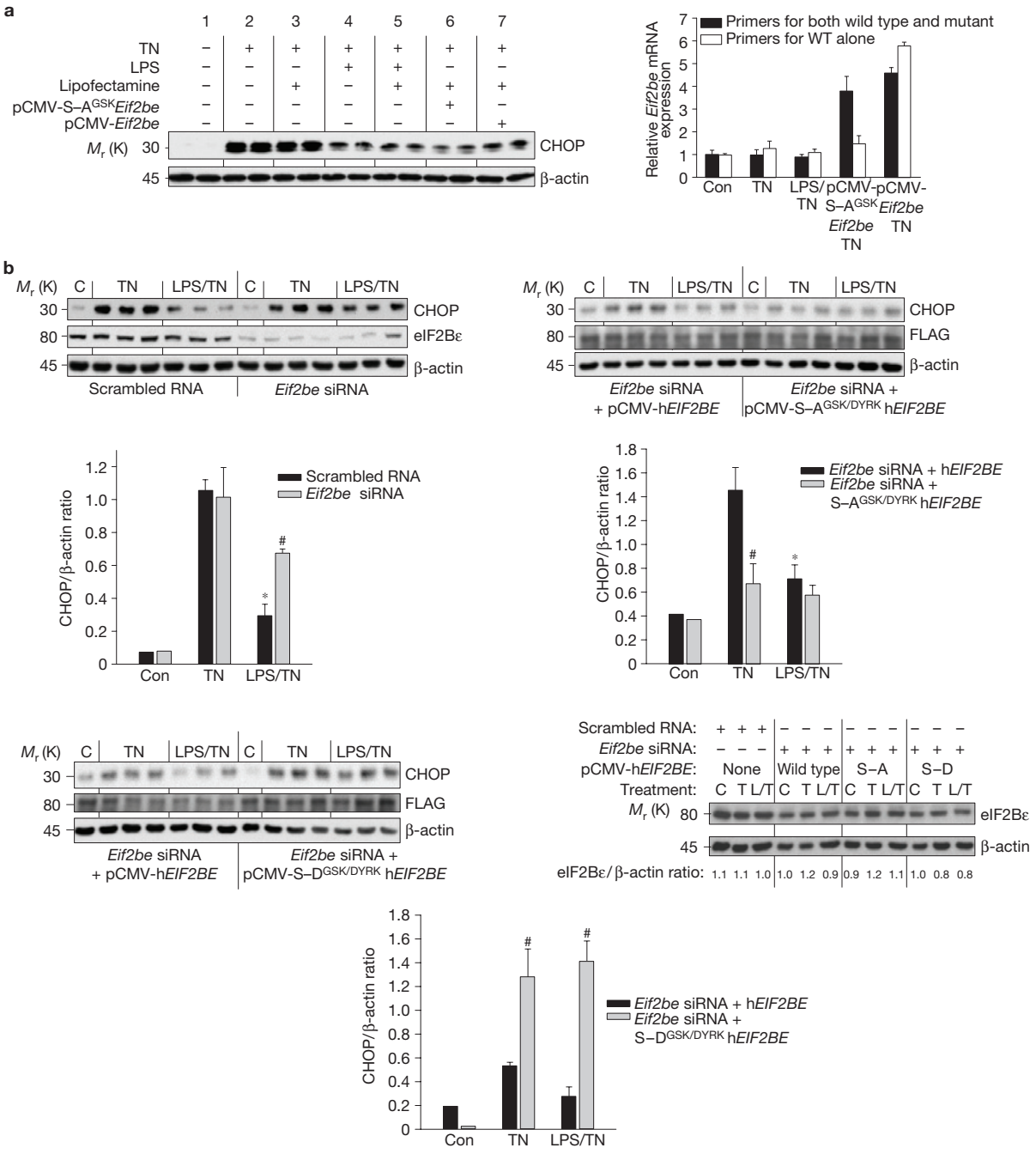

Figure 2 Evidence that dephosphorylation of eIF2Bε is involved in LPS-mediated CHOP suppression in ER-stressed MEFs. (**a**) MEFs were treated under the indicated conditions, and then cell extracts were analysed by immunoblot for CHOP and β-actin (left). The conditions were the same as those in Supplementary Fig. S1a (8 h with or without LPS then 2 h tunicamycin) except that the cells in lanes 3 and 5 first underwent mock transfection (Lipofectamine) and those in 6 and 7 were transfected with plasmids encoding rat *Eif2be* with a serine–alanine mutation in the GSK3β phospho-site (S–A^{GSK}) or wild-type *Eif2be*. The histogram (right) shows the levels of total (black bars) and wild-type-alone (white bars) *Eif2be* mRNA from MEFs incubated under the indicated conditions. The mRNA data are from triplicate samples from the groups shown in the left panel, and expressed as mean ± s.e.m. with $n = 3$. Con, untreated group; TN, tunicaymcin (1 mg ml^{-1}). (**b**) In the upper left panel, MEFs were transfected with scrambled RNA or murine *Eif2be* siRNA, and in the upper right and lower left immunoblot panels, *Eif2be*-silenced MEFs were then transfected with a plasmid encoding wild-type human eIF2Bε or human eIF2Bε with serine–alanine (upper right) or serine–aspartic acid (lower left) mutations in the GSK and DYRK sites (S–A$^{GSK/DYRK}$ and S–D$^{GSK/DYRK}$, respectively). At 12 h after transfection with the wild-type or mutant h*EIF2BE* plasmids, the cells were pre-treated for 8 h in the absence or presence of LPS (500 ng ml^{-1}) and then incubated for 2 h in control medium (C) or in medium containing tunicamycin (TN, 0.5 μg ml^{-1}). Extracts were subjected to immunoblot analysis for CHOP, eIF2Bε or FLAG, and β-actin. Densitometric quantification of the immunoblot data is shown in the histograms as mean ± s.e.m. with $n = 3$. $^{*}P < 0.05$ versus the TN group; $^{\#}P < 0.05$ versus scrambled RNA (upper left) or versus wild-type h*EIF2BE* groups (upper right and lower left histograms). Lower right immunoblot, total eIF2Bε (with β-actin as a loading control) in samples from the experiments in the upper left and lower left panels; densitometric quantification of each lane appears below that lane. C, control; L, LPS; T, tunicamycin. Uncropped images of blots are shown in Supplementary Fig. S6.

site and an upstream serine residue, which, when phosphorylated by the kinase DYRK, promotes phosphorylation of the GSK site[8,9] (S–A$^{GSK/DYRK}$). This mutant, which cannot be phosphorylated, should be in a constitutively active state that should promote 'resistance' to p-eIF2α and thereby blunt ER-stress-induced CHOP induction (see Fig. 2a). Most importantly, if LPS suppresses CHOP by decreasing the level of eIF2Bε phosphorylation, it should have little effect in these cells, because, in the absence of phosphorylation, the mutant cannot be dephosphorylated. The data bear out this prediction: compared with MEFs transfected with wild-type h*EIF2BE*, those transfected with S–A$^{GSK/DYRK}$ h*EIF2BE* showed a lower level of CHOP expression in response to tunicamycin and no significant further decrease in the CHOP level with LPS pre-treatment (Fig. 2b, upper right). Finally, using serine–aspartic acid mutants to mimic constitutive phosphorylation, we showed that transfection with S–D$^{GSK/DYRK}$ EIF2BE did not restore LPS-induced CHOP suppression in *Eif2be*-silenced MEFs (Fig. 2b, lower left). Note that the level of total eIF2Bε in cells with silenced endogenous protein plus transfected human protein was similar to the level of endogenous eIF2Bε in non-silenced, non-transfected cells (Fig. 2b, lower right). These combined data provide further evidence that eIF2Bε dephosphorylation plays an important role in LPS-mediated suppression of CHOP in ER-stressed cells.

In theory, LPS could lead to a decreased level of p-eIF2Bε by decreasing GSK3 activity. However, we found that LPS did not increase the level of the inactive phosphorylated form of GSK3β (Supplementary Fig. S2a) or GSK3α. Moreover, treatment with the phosphatidylinositol-3-OH kinase inhibitor LY294002, which activates GSK3β (ref. 11), did not prevent the LPS-mediated suppression of CHOP (data not shown). These data indicated that a phosphatase might be involved, which we investigated by incubating cell extracts with [^{32}P]eIF2Bε and monitoring the rate of ^{32}P dephosphorylation. LPS treatment enhanced the level of dephosphorylation in wild-type but not *Trif*$^{-/-}$ macrophages (Fig. 3a). Moreover, the enhanced level of dephosphorylation was suppressed by the phosphatase inhibitor okadaic acid (Fig. 3a) but not by inhibitors of MAPK phosphatase 1, PP1 and PP2B (data not shown). As okadaic acid can inhibit PP2A, we tested the effect of siRNA-mediated silencing of the catalytic 'C' subunit of PP2A. Compared with scrambled RNA, *Pp2ac* siRNA prevented the LPS-mediated decrease in both p-eIF2Bε and CHOP levels in ER-stressed macrophages (Fig. 3b). Note that *Pp2ac* siRNA also prevented the LPS-mediated decrease in the level of ATF4 (Supplementary Fig. S2b), which we showed previously is the most proximal translational target of the 'p-eIF2α resistance' pathway[3]. Finally, we found that a constitutively active mutant of PP2A with a Y307F mutation in the catalytic subunit[12] was able to mimic the effect of LPS on suppression of CHOP (Fig. 3c, left). Conversely, a dominant-negative mutant with an L199P mutation in the catalytic subunit[13] prevented LPS-mediated CHOP suppression (Fig. 3c, right). These combined results provide evidence for a pathway in which LPS pre-treatment of ER-stressed cells activates PP2A-mediated dephosphorylation of eIF2Bε, resulting in suppression of CHOP.

PP2A can be activated by an increase in the expression of one or more of its three subunits; a decrease in the association of PP2Ac with the inhibitors ANP32 or α-4 (refs 14,15); or dephosphorylation of the catalytic subunit at Tyr 307 (ref. 16). LPS pre-treatment did not affect the expression of any of the PP2A subunits or association of PP2Ac with ANP32 or α-4 (data not shown). However, LPS pre-treatment led to a subtle but reproducible and statistically significant decrease in pTyr307-PP2Ac in wild-type but not *Trif*$^{-/-}$ macrophages (Fig. 3d). To investigate this point *in vivo*, we took advantage of the fact that LPS pre-treatment of tunicamycin-treated mice suppresses CHOP expression, but not eIF2α phosphorylation, in the liver and kidney in a TRIF-dependent manner[3]. We found that LPS pre-treatment led to a decrease in the levels of p-eIF2Bε and p-PP2Ac in liver and kidney extracts of tunicamycin-treated mice (Fig. 3e,f), similar to our observations in cultured macrophages and MEFs.

Src-family kinases (SFKs) can phosphorylate PP2Ac at Tyr 307 and thereby inhibit PP2A phosphatase activity[16–18], and so a decrease in SFK activity could be a mechanism of PP2A activation. Consistent with this possibility, we found that LPS partially decreased the level of phospho-Tyr-p60$^{c\text{-}src}$ (p-Src), a measure of Src activation[19], in wild-type but not *Trif*$^{-/-}$ macrophages (Fig. 4a) and inhibited the kinase activity of immunoprecipitated Src (Fig. 4b). Poly(I:C), a ligand for the TLR3–TRIF pathway that is a potent suppressor of CHOP in ER-stressed macrophages[3], also promoted the dephosphorylation of both Src and PP2Ac (Supplementary Fig. S2c). To determine causation, we investigated the effect of a phosphopeptide (EPQ[pY]EEIPIYL) that activates SFKs by binding to and inhibiting their auto-inhibitory SH2 domains[20,21] and found that it abrogated LPS-induced suppression of both p-PP2Ac and CHOP without increasing the level of p-eIF2α (Fig. 4c). The changes in CHOP protein seen with LPS and Src activator treatment were paralleled by changes in *Chop* mRNA (Fig. 4c, bottom right), which is consistent with the fact that the overall pathway involves ATF4-induced *Chop* mRNA (ref. 3). Moreover, the 'p-eIF2α resistance' hypothesis predicts that activation of SFKs would prevent LPS-induced enhancement of global translation in ER-stressed cells[3]. Indeed, by quantifying newly synthesized [^{35}S]-labelled proteins, we found that the SFK peptide activator abrogated the LPS-induced increment in the level of new protein translation in tunicamycin-treated macrophages (Fig. 4d).

To determine whether SFK inhibition could mimic the effect of LPS, ER-stressed cells were treated with the SFK inhibitors PP1 or Su6656, and each was found to suppress p-PP2Ac and CHOP in the absence of LPS (Fig. 4e). Similar data were obtained using immunofluorescence microscopy assays: LPS treatment led to a decrease in the level of the p-Src signal in wild-type but not *Trif*$^{-/-}$ macrophages either in the absence or presence of tunicamycin (Supplementary Fig. S2d,e), and both LPS and PP1 decreased the level of the p-PP2Ac signal in tunicamycin-treated cells (Supplementary Fig. S2f). As further evidence for the role of SFKs in the pathway, we found that CHOP suppression by the SFK inhibitors was lessened substantially by *Pp2ac* silencing (Supplementary Fig. S3a), indicating that this action of the SFK inhibitors requires PP2Ac. Moreover, MEFs transfected with a dominant-negative form of Src (K296R-Y528F) that acts as a pan-SFK inhibitor[22] mimicked the ability of LPS to suppress tunicamycin-induced CHOP expression (Supplementary Fig. S3b). This construct also suppressed hepatic p-PP2Ac, p-eIF2Bε and CHOP when introduced into the tunicamycin mouse model described above (Supplementary Fig. S3c). These combined data provide strong support for the role of SFK inhibition in the TLR–PP2A–eIF2Bε–CHOP pathway.

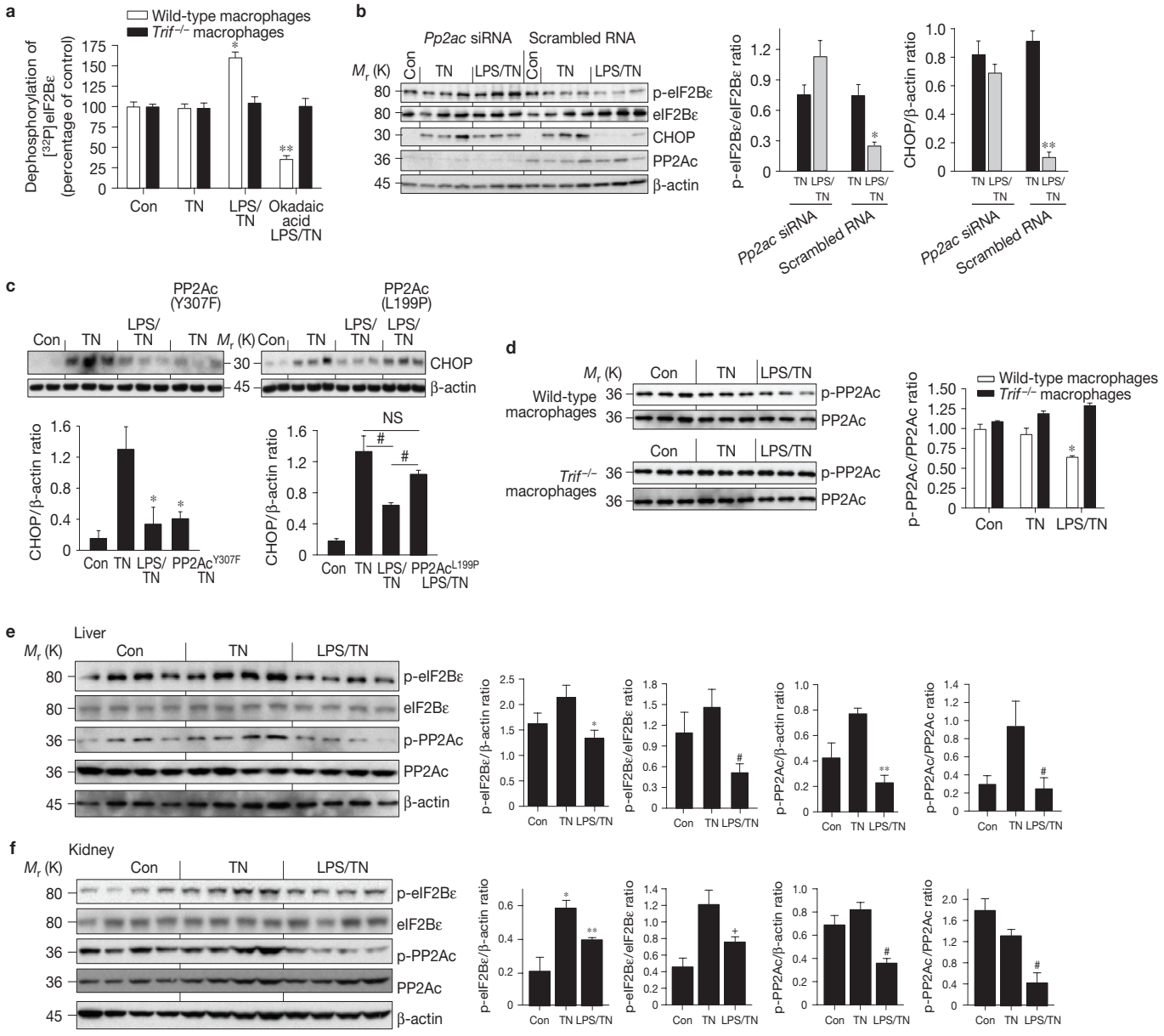

Figure 3 LPS promotes dephosphorylation of eIF2Bε through a mechanism involving PP2A, with evidence *in vivo*. (**a**) Macrophages from wild-type or *Trif*$^{-/-}$ mice were untreated (Con) or pre-treated (or not) with LPS (1 ng ml^{-1}) for 24 h followed by treatment with tunicamycin (TN, 1 μg ml^{-1}) for 90 min. In an additional LPS/TN group, the phosphatase inhibitor okadaic acid (1 nM) was added at the same time as LPS. Cell extracts were then added to a solution of purified ^{32}P-labelled eIF2Bε, and the rate of dephosphorylation was determined as described in the Methods. Data are expressed as mean ± s.e.m. with $n = 6$; $^{*}P < 0.05$, compared with the control (Con) and the corresponding *Trif*$^{-/-}$ group. $^{**}P < 0.05$, compared with the TN group and the corresponding *Trif*$^{-/-}$ group. (**b**) Macrophages were transfected with scrambled RNA or *Pp2ac* siRNA, and 48 h later the cells were treated similarly to the first three wild-type groups in **a**. Cell extracts were analysed by immunoblot (left) for p-eIF2Bε and total eIF2Bε, CHOP, PP2Ac and β-actin. The data were then quantified by densitometry (right). $^{*}P < 0.05$ and $^{**}P < 0.02$ versus the TN group in the scrambled RNA groups. (**c**) MEFs were either mock-transfected or transfected with a plasmid encoding PP2Ac with a Tyr307–phenylalanine mutation or a Leu199–proline mutation. At 12 h post-transfection, cells were then treated ±LPS (500 ng ml^{-1}) for 8 h followed by a 2 h treatment with tunicamycin (0.5 μg ml^{-1}). Cell extracts were subjected to immunoblot analysis for CHOP and β-actin (top). Densitometric quantification of the immunoblot data is shown in the histograms (bottom). $^{*}P < 0.001$ versus the TN group; $^{\#}P < 0.03$ versus the LPS/TN group; NS, not significant. (**d**) Macrophages from wild-type or *Trif*$^{-/-}$ mice were untreated (Con) or pre-treated (or not) with LPS (1 ng ml^{-}1) for 24 h followed by treatment with tunicamycin (1 μg ml^{-1}) for 3 h. Extracts were analysed by immunoblot for p-PP2Ac and total PP2Ac (left) and then quantified by densitometry (right); $^{*}P < 0.05$ versus the control and TN groups for wild-type macrophages and versus all groups for *Trif*$^{-/-}$ macrophages. (**e**) Mice were injected intravenously with LPS (80 μg kg^{-1}) or vehicle control once a day for 2 consecutive days and then injected with tunicamycin (1 mg kg^{-1}) intraperitoneally. Twelve hours later, the mice were killed, and liver extracts were assayed by immunoblot for p-PP2Ac and total PP2Ac, p-eIF2Bε and total eIF2Bε, and β-actin (left) and then quantified by densitometry (right). $^{*}P = 0.04$; $^{**}P = 0.0004$; $^{\#}P = 0.015$. (**f**) The same as in **e**, except the mice were killed 24 h after the tunicamycin injection, and kidney extracts were assayed. $^{*}P = 0.02$, compared with the control; $^{**}P = 0.04$, compared with the TN group. $^{+}P < 0.05$, compared with the TN group; $^{\#}P < 0.01$, compared with the TN group. All densitometry data are expressed as mean ± s.e.m. with $n = 3$, except $n = 4$ for **e** and **f**. Uncropped images of blots are shown in Supplementary Fig. S6.

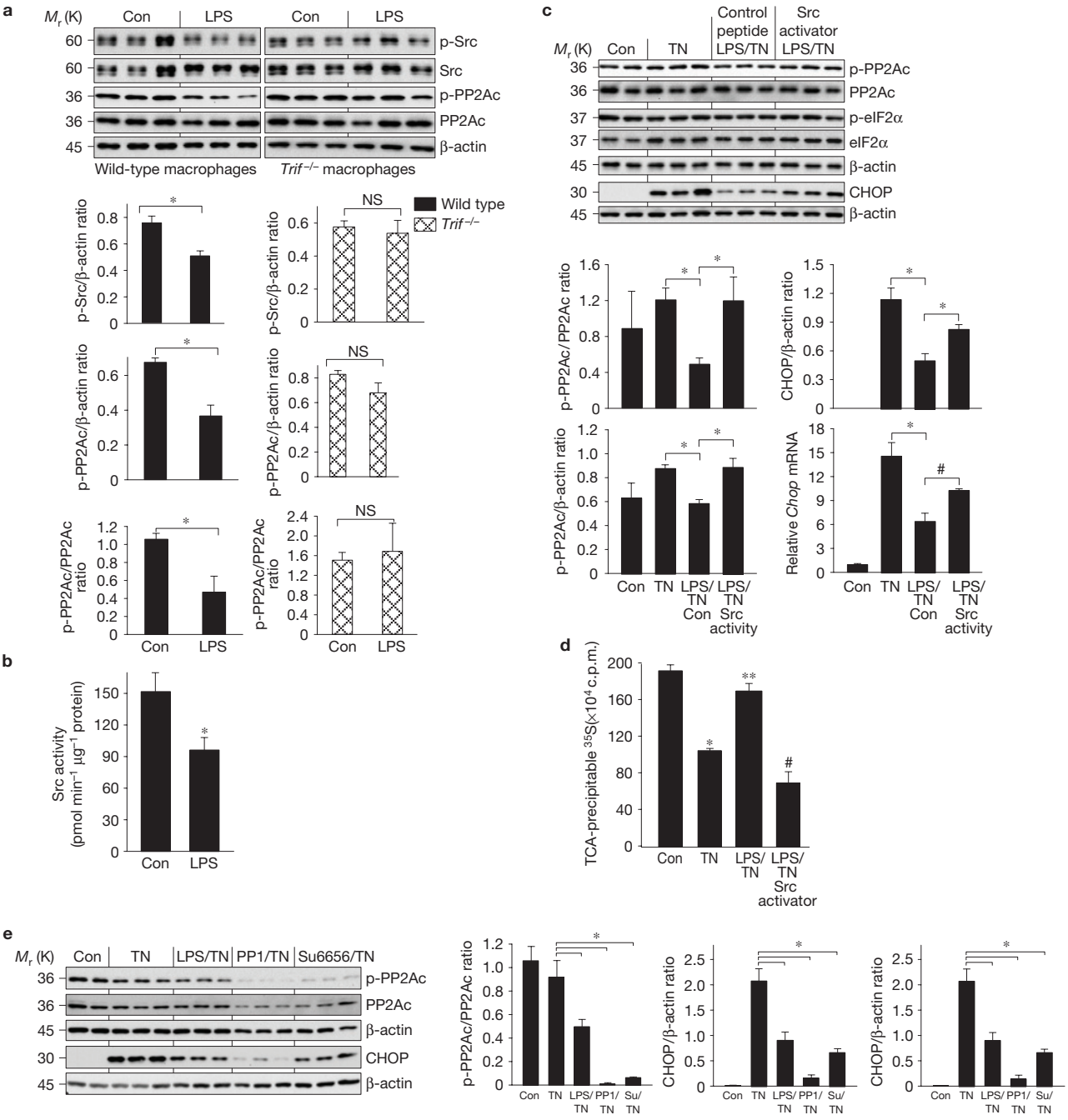

Figure 4 Evidence that TLR–TRIF-mediated PP2Ac dephosphorylation, CHOP suppression and restoration of global protein translation involve a pathway involving SFK deactivation. (**a**) Macrophages from wild-type or *Trif*$^{-/-}$ mice were untreated (Con) or treated with LPS (1 ng ml^{-1}) for 24 h. Extracts were analysed by immunoblot for pTyr 416 and total Src, p-PP2Ac and total PP2Ac, and β-actin (top) and then quantified by densitometry (bottom). $n = 3$; $^{*}P < 0.03$. NS, not significant. (**b**) Src was immunoprecipitated from cell extracts of control or LPS-treated macrophages and its kinase activity was then assayed. $n = 4$; $^{*}P < 0.05$. (**c**) Macrophages were untreated or pre-treated (or not) with LPS (1 ng ml^{-1}) for 24 h followed by treatment with tunicamycin (TN, 1 μg ml^{-1}) for 3 h for PP2Ac, 7 h for CHOP protein or 5 h for *Chop* mRNA. The LPS/TN or TN groups were pre-treated for 4 h before the above incubations with or without control peptide or Src activator peptide under conditions that facilitated their uptake by the cells (Methods). Extracts were analysed by immunoblot for p-PP2Ac and total PP2Ac, p-eIF2α and total eIF2α, CHOP and β-actin (top) and then quantified by densitometry (bottom). $n = 3$; $^{*}P < 0.05$. *Chop* mRNA was assayed by real-time quantitative PCR. $n = 3$; $^{*}P = 0.015$; $^{\#}P = 0.04$. (**d**) Macrophages were treated under control (Con), TN, LPS/TN or LPS/TN/Src activator conditions as above. The cells were then pulse-labelled with [^{35}S]methionine-cysteine for 20 min, followed by precipitation with ice-cold TCA and then quantification of ^{35}S c.p.m. in the TCA precipitate. $n = 4$; $^{*}P < 0.05$, compared with the control; $^{**}P < 0.05$, compared with the TN group; $^{\#}P < 0.05$, compared with the LPS/TN group. (**e**) Macrophages were untreated or pre-treated (or not) with LPS (1 ng ml^{-1}) for 24 h followed by treatment with tunicamycin (1 μg ml^{-1}) for 3 h (for PP2Ac) or 7 h (for CHOP). Some of the tunicamycin-treated cells were co-treated with the SFK inhibitors PP1 (10 μM) or Su6656 (Su; 20 μM). Extracts were analysed by immunoblot for p-PP2Ac and total PP2Ac, CHOP and β-actin (left) and then quantified by densitometry (right). $n = 3$; $^{*}P < 0.05$. All data are expressed as mean ± s.e.m. with n as indicated above. Uncropped images of blots are shown in Supplementary Fig. S6.

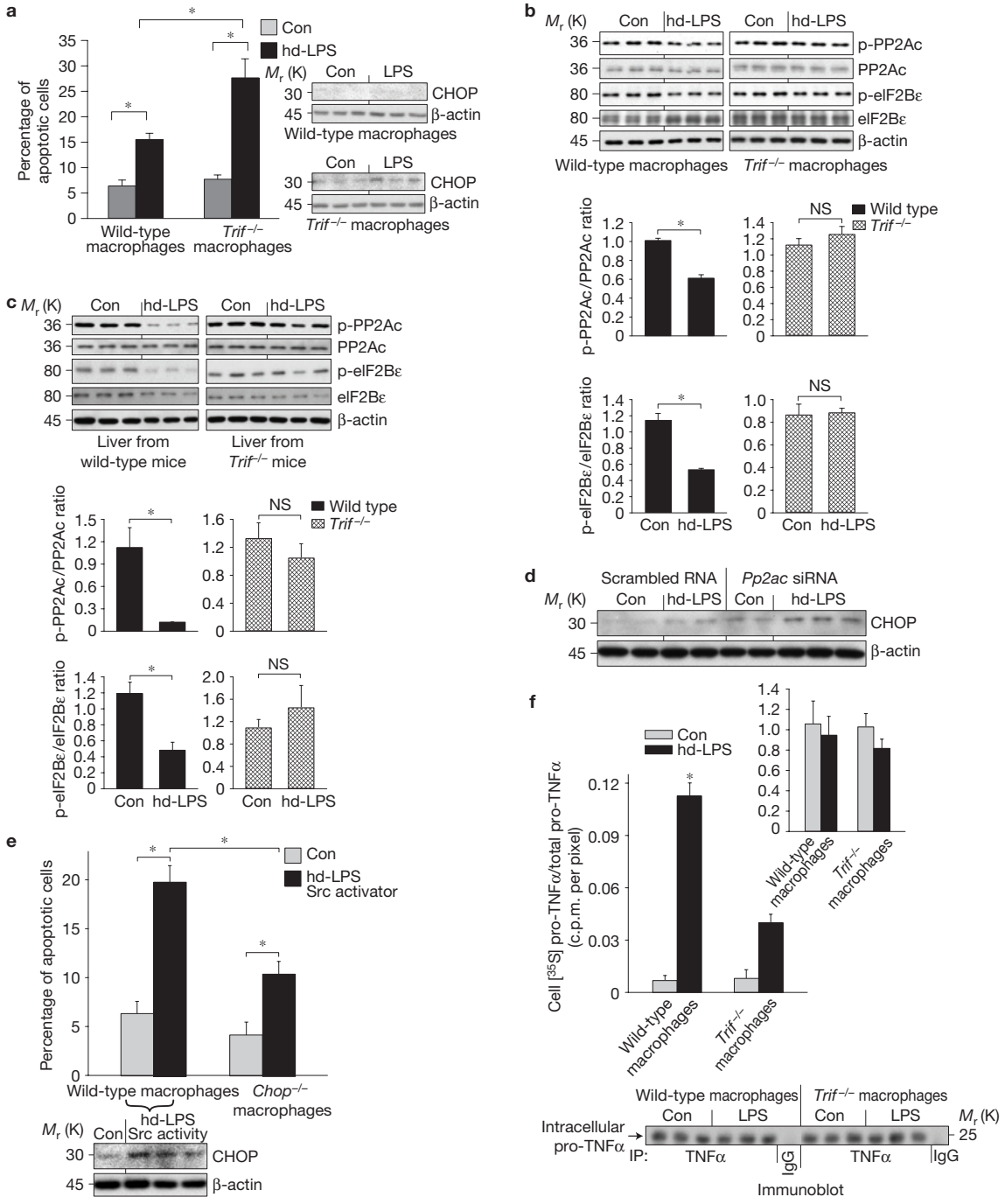

Figure 5 Evidence for and functional significance of the TRIF–Src–PP2Ac–eIF2B pathway in an hd-LPS model. (**a**) Macrophages from wild-type and *Trif*$^{-/-}$ mice were treated for 24 or 28 h in the absence (Con) or presence of hd-LPS (1 μg ml^{-1}). The cells were then assayed for apoptosis (28 h) or CHOP and β-actin expression (24 h). $^{*}P < 0.05$. (**b**) Additional extracts from the 24 h cells in **a** were analysed by immunoblot for p-PP2Ac and total PP2Ac, p-eIF2α and total eIF2Bε, and β-actin (top) and quantified by densitometry (bottom). $^{*}P < 0.02$; NS, not significant. Similar densitometry data were obtained using β-actin as a loading control (not shown). (**c**) Wild-type or *Trif*$^{-/-}$ mice were injected intraperitoneally with PBS control or 5 mg kg^{-1} LPS (hd-LPS). Three hours later, liver extracts were assayed for p-PP2Ac and total PP2Ac, p-eIF2Bε and total eIF2Bε, and β-actin by immunoblot (top) and quantified by densitometry (bottom). $^{*}P < 0.02$; NS, not significant. (**d**) Macrophages were transfected with scrambled RNA or *Pp2ac* siRNA, and 48 h later the cells were treated with hd-LPS (1 μg ml^{-1}). Extracts were subjected to immunoblot analysis for CHOP and β-actin. (**e**) Macrophages from wild-type and *Trif*$^{-/-}$ mice were treated under control conditions or with hd-LPS (1 μg ml^{-1}) at time = 0 and then the Src activator peptide used in Fig. 4c was added at time = 10 h. At time = 24 h, the cells were assayed for apoptosis ($n = 3$ per group), and extracts from parallel incubations were analysed by immunoblot for CHOP and β-actin. $^{*}P < 0.01$. (**f**) Macrophages from wild-type and *Trif*$^{-/-}$ mice were first treated for a total of 16 h in the absence (Con) or presence of hd-LPS (1 μg ml^{-1}), where the last hour included [^{35}S]methionine-cysteine in the medium. Cell extracts were immunoprecipitated using anti-TNFα or IgG control, followed by approximate equal loading of immunoprecipitated TNFα and then anti-TNFα immunoblot. The pro-TNFα band (M_r 25K) for each sample on the immunoblot was quantified by densitometry (each band was assigned a pixel value), and then the bands were cut out and their [^{35}S] c.p.m. was counted. The data were quantified as c.p.m. per pixel. $^{*}P = 0.01$ versus all other groups. Inset histogram, *Tnfa* mRNA level at the 16 h time point. All data are expressed as mean ± s.e.m. with $n = 3$. Uncropped images of blots are shown in Supplementary Fig. S7.

We speculate that this TRIF–CHOP suppression pathway protects cells from CHOP-induced apoptosis during LPS-induced sepsis. Indeed, when the pathway is disabled by TRIF deficiency in high-dose (hd) LPS-treated mice, where hd-LPS is both the inducer of ER stress and the activator of the TLR–TRIF–CHOP suppression pathway, we observed an elevated level of CHOP, cell death and organ dysfunction in spleen, liver and kidney[3]. In hd-LPS-treated macrophages, where CHOP expression and apoptosis were suppressed in wild-type but not *Trif*$^{-/-}$ macrophages (Fig. 5a), the level of phosphorylation of PP2Ac, eIF2Bε and Src was subtly but reproducibly reduced in a TRIF-dependent manner (Fig. 5b and Supplementary Fig. S4a–c). Moreover, hd-LPS treatment of wild-type, but not *Trif*$^{-/-}$, mice caused a marked decrease in the level of both p-PP2Ac and p-eIF2Bε in liver (Fig. 5c) and kidney (data not shown). As tests of causation, we found that *Pp2ac* siRNA and Src activator peptide increased the level of CHOP expression in hd-LPS-treated macrophages, and the Src activator also increased the level of CHOP-dependent apoptosis (Fig. 5d,e).

We reason that the pathway also maintains uninterrupted synthesis of key proteins needed for a proper LPS-induced inflammatory response by promoting 'resistance' to the translational inhibitory effect of p-eIF2α (see Fig. 4d). We first showed that TRIF deficiency blocked the hd-LPS-induced increase in secreted, immunoreactive stimulated TNFα (Supplementary Fig. S4d). To distinguish between transcriptional and translational regulation, we conducted a [^{35}S]methionine-cysteine labelling experiment and found that hd-LPS increased the level of labelled [^{35}S]TNFαin the medium of wild-type but not *Trif*$^{-/-}$ macrophages (Supplementary Fig. S4e). This result cannot be explained by a decreased level of processing or secretion of TNFα in *Trif*$^{-/-}$ macrophages, because approximately equal amounts of immunoprecipitated TNFα protein were loaded in each lane of the gel. Most importantly, when we directly examined newly translated TNFα by conducting a short-term labelling experiment at a time when *Tnfa* mRNA levels were similar among all groups (Fig. 5f inset), we found a marked decrease in the level of newly translated pro-TNFα. Together, these data support the idea that the TRIF pathway described herein enables uninterrupted translation of *Tnfa* mRNA.

The data in this report provide evidence for an eIF2B dephosphorylation–GEF activation pathway that initially involves SFK de-activation and then PP2A activation (Supplementary Fig. S5). We reason that activation of eIF2B by this pathway boosts the level of GTP exchange on eIF2 enough to enable proper ternary complex cycling despite the presence of p-eIF2α (refs 8,23). One possibility is that ε-dephosphorylated eIF2B can exchange GDP for GTP with higher-than-normal efficiency on the subpopulation of eIF2 complexes whose α-subunit escapes PERK-mediated phosphorylation, thus compensating for the translation-inhibitory and CHOP-inducing effects of the eIF2 complexes whose α-subunit is phosphorylated. Another possibility is that dephosphorylated eIF2B could carry out its GEF function on eIF2 complexes that do have α-subunit phosphorylation, for example, through a conformation change in dephosphorylated eIF2B that might increase its off-rate from the inhibitory site on p-eIF2α and thus enable GDP–GTP exchange on the γ-subunit of eIF2. Regardless of mechanism, restoration of protein translation initiation would both suppress the level of ATF4–CHOP and maintain a normal rate of global protein translation. To the extent that the pathway enables LPS-activated macrophages to carry out essential protein translation, it probably works in concert with complementary LPS-induced mechanisms that enhance translation initiation, such as mTOR-induced phosphorylation of 4E-BP1, which activates the initiation factor eIF4E (ref. 24).

The mechanism of SFK deactivation by TLR–TRIF signalling will require further investigation, but our previous findings indicate that IRF5 and IRF7, but not IRF3, should have a role[3]. Interestingly, other studies have reported that LPS can activate SFKs, which, on the basis of the use of chemical inhibitors of SFKs in these reports, may be involved in certain LPS signalling pathways[25–27]. However, these studies are distinguished from the one here by their use of a much shorter LPS incubation time (30 min versus 14–24 h here). We found that the minimum LPS pre-incubation time that decreased the level of pTyr416-Src was 8 h, which is consistent with the time of LPS pre-treatment required for CHOP suppression[3]. This lag time may reflect the signalling events downstream of TLR–TRIF needed for LPS or poly(I:C) to induce the change in SFK activity. Moreover, previous studies in this area used an immortalized cell line derived from a leukaemia-virus-induced tumour (RAW 264.7) or retrovirus-immortalized bone marrow cells instead of primary macrophages. We found that ER-stressed tumour-cell-derived cell lines, including RAW 264.7 cells, are not responsive to the CHOP-suppressive effect of pathophysiologic relevant doses of LPS (C.W. Woo and I. Tabas, unpublished observations).

Future investigations will examine the relevance of this pathway to advanced atherosclerosis, where CHOP-induced macrophage apoptosis promotes plaque necrosis, a key feature of clinically dangerous plaques[28]. In advanced atherosclerotic lesions, the level of macrophage CHOP expression is very high despite the presence of numerous TLR ligands and evidence of macrophage TLR–TRIF activation[28,29]. Therefore, we speculate that the CHOP-suppressive pathway becomes disabled in this setting, perhaps owing to interruption of one of the signalling components identified herein. Conversely, tumour cells, which often show evidence of UPR activation without UPR-induced apoptosis, can be become resistant to the protein-translation-inhibiting effects of p-eIF2α in the absence of LPS (ref. 30). In one study with human breast cancer cells, this process was associated with an increase in the amount of eIF2B protein[31], but it is possible that activation of eIF2Bε by dephosphorylation might play a role in 'p-eIF2α resistance' in other types of cancer cell. If so, strategies to disable eIF2B GEF-activating pathways that render cells resistant to p-eIF2α, such as the one described here, may decrease the resistance of certain types of cancer cell to ER-stress-induced cell death[32]. Thus, with further knowledge of the pathway described here, pharmacologic manipulation in one direction or the other may have unique therapeutic potential. □

METHODS

Methods and any associated references are available in the online version of the paper at http://www.nature.com/naturecellbiology

Note: Supplementary Information is available on the Nature Cell Biology website

ACKNOWLEDGEMENTS

This work was supported by postdoctoral fellowship grants from the Canadian Institutes of Health Research and the Heart & Stroke Foundation of Canada (C.W.W.); NIH-NHLBI grants HL75662 and HL57560 (I.T.); and NIH-NIDDK grants DK13499 and DK15658 (S.R.K.). We thank D. Ron (University of Cambridge, UK) for helpful discussions and for providing the CHOP–GFP reporter plasmid;

C. Proud (University of Southampton, UK) for recombinant GST–DYRK2; D. Ren (University of Pennsylvania, USA) for advice regarding the use of mutant Src constructs; D. L. Brautigan (University of Virginia School of Medicine, USA) for the construct encoding $PP2Ac^{Y307F}$; B. A. Hemmings (Friedrich Miescher Institute, Basel, Switzerland) for the construct encoding $PP2Ac^{L199P}$; and B. Berk (University of Rochester, USA) for an adenoviral vector encoding kinase-inactive Src.

AUTHOR CONTRIBUTIONS

C.W.W. carried out the experiments and assisted with planning the experiments, data analysis and writing the manuscript; L.K. assisted with planning the experiments and data analysis; S.R.K. assisted with planning the experiments, data analysis and writing the manuscript; I.T. coordinated the project and assisted with planning the experiments, data analysis and writing the manuscript.

COMPETING FINANCIAL INTERESTS

The authors declare no competing financial interests.

Published online at http://www.nature.com/naturecellbiology
Reprints and permissions information is available online at http://www.nature.com/reprints

1. Todd, D. J., Lee, A. H. & Glimcher, L. H. The endoplasmic reticulum stress response in immunity and autoimmunity. *Nat. Rev. Immunol.* **8,** 663–674 (2008).
2. Ron, D. & Walter, P. Signal integration in the endoplasmic reticulum unfolded protein response. *Nat. Rev. Mol. Cell Biol.* **8,** 519–529 (2007).
3. Woo, C. W. *et al.* Adaptive suppression of the ATF4-CHOP branch of the unfolded protein response by toll-like receptor signalling. *Nat. Cell Biol.* **11,** 1473–1480 (2009).
4. Ron, D. Translational control in the endoplasmic reticulum stress response. *J. Clin. Invest.* **110,** 1383–1388 (2002).
5. Tabas, I. & Ron, D. Molecular mechanisms integrating pathways of endoplasmic reticulum stress-induced apoptosis. *Nat. Cell Biol.* **13,** 184–190 (2011).
6. Oyadomari, S. & Mori, M. Roles of CHOP/GADD153 in endoplasmic reticulum stress. *Cell Death. Differ.* **11,** 381–389 (2004).
7. Krishnamoorthy, T., Pavitt, G. D., Zhang, F., Dever, T. E. & Hinnebusch, A. G. Tight binding of the phosphorylated α subunit of initiation factor 2 (eIF2α) to the regulatory subunits of guanine nucleotide exchange factor eIF2B is required for inhibition of translation initiation. *Mol. Cell Biol.* **21,** 5018–5030 (2001).
8. Welsh, G. I., Miller, C. M., Loughlin, A. J., Price, N. T. & Proud, C. G. Regulation of eukaryotic initiation factor eIF2B: glycogen synthase kinase-3 phosphorylates a conserved serine which undergoes dephosphorylation in response to insulin. *FEBS Lett.* **421,** 125–130 (1998).
9. Wang, X. & Proud, C. G. A novel mechanism for the control of translation initiation by amino acids, mediated by phosphorylation of eukaryotic initiation factor 2B. *Mol. Cell Biol.* **28,** 1429–1442 (2008).
10. Hardt, S. E., Tomita, H., Katus, H. A. & Sadoshima, J. Phosphorylation of eukaryotic translation initiation factor 2Bε by glycogen synthase kinase-3β regulates β-adrenergic cardiac myocyte hypertrophy. *Circ. Res.* **94,** 926–935 (2004).
11. Fang, X. *et al.* Phosphorylation and inactivation of glycogen synthase kinase 3 by protein kinase A. *Proc. Natl Acad. Sci. USA* **97,** 11960–11965 (2000).
12. Chung, H., Nairn, A. C., Murata, K. & Brautigan, D. L. Mutation of Tyr307 and Leu309 in the protein phosphatase 2A catalytic subunit favors association with the α 4 subunit which promotes dephosphorylation of elongation factor-2. *Biochemistry* **38,** 10371–10376 (1999).
13. Evans, D. R., Myles, T., Hofsteenge, J. & Hemmings, B. A. Functional expression of human PP2Ac in yeast permits the identification of novel C-terminal and dominant-negative mutant forms. *J. Biol. Chem.* **274,** 24038–24046 (1999).
14. Santa-Coloma, T. A. Anp32e (Cpd1) and related protein phosphatase 2 inhibitors. *Cerebellum* **2,** 310–320 (2003).
15. Nanahoshi, M. *et al.* α4 protein as a common regulator of type 2A-related serine/threonine protein phosphatases. *FEBS Lett.* **446,** 108–112 (1999).
16. Chen, J., Martin, B. L. & Brautigan, D. L. Regulation of protein serine–threonine phosphatase type-2A by tyrosine phosphorylation. *Science* **257,** 1261–1264 (1992).
17. Hu, X. *et al.* Src kinase up-regulates the ERK cascade through inactivation of protein phosphatase 2A following cerebral ischemia. *BMC. Neurosci.* **10,** 74 (2009).
18. Barisic, S., Schmidt, C., Walczak, H. & Kulms, D. Tyrosine phosphatase inhibition triggers sustained canonical serine-dependent NFκB activation via Src-dependent blockade of PP2A. *Biochem. Pharmacol.* **80,** 439–447 (2010).
19. Brown, M. T. & Cooper, J. A. Regulation, substrates and functions of src. *Biochim. Biophys. Acta* **1287,** 121–149 (1996).
20. Liu, X. *et al.* Regulation of c-Src tyrosine kinase activity by the Src SH2 domain. *Oncogene* **8,** 1119–1126 (1993).
21. Lu, B. *et al.* Peptide neurotransmitters activate a cation channel complex of NALCN and UNC-80. *Nature* **457,** 741–744 (2009).
22. Encinas, M. *et al.* c-Src is required for glial cell line-derived neurotrophic factor (GDNF) family ligand-mediated neuronal survival via a phosphatidylinositol-3 kinase (PI-3K)-dependent pathway. *J. Neurosci.* **21,** 1464–1472 (2001).
23. Mayhew, D. L., Hornberger, T. A., Lincoln, H. C. & Bamman, M. M. Eukaryotic initiation factor 2Bε induces cap-dependent translation and skeletal muscle hypertrophy. *J. Physiol.* **589,** 3023–3037 (2011).
24. Potter, M. W., Shah, S. A., Elbirt, K. K. & Callery, M. P. Endotoxin (LPS) stimulates 4E-BP1/PHAS-I phosphorylation in macrophages. *J. Surg. Res.* **97,** 54–59 (2001).
25. Lee, J. Y. *et al.* The regulation of the expression of inducible nitric oxide synthase by Src-family tyrosine kinases mediated through MyD88-independent signaling pathways of Toll-like receptor 4. *Biochem. Pharmacol.* **70,** 1231–1240 (2005).
26. Kim, J. Y. *et al.* Src-mediated regulation of inflammatory responses by actin polymerization. *Biochem. Pharmacol.* **79,** 431–443 (2010).
27. Tu, S., Wu, W. J., Wang, J. & Cerione, R. A. Epidermal growth factor-dependent regulation of Cdc42 is mediated by the Src tyrosine kinase. *J. Biol. Chem.* **278,** 49293–49300 (2003).
28. Moore, K. J. & Tabas, I. Macrophages in the pathogenesis of atherosclerosis. *Cell* **145,** 341–355 (2011).
29. Curtiss, L. K. & Tobias, P. S. Emerging role of toll-like receptors in atherosclerosis. *J. Lipid Res.* **50 Suppl,** S340–S345 (2008).
30. Lee, A. S. & Hendershot, L. M. ER stress and cancer. *Cancer Biol. Ther.* **5,** 721–722 (2006).
31. Check, J. *et al.* Src kinase participates in LPS-induced activation of NADPH oxidase. *Mol. Immunol.* **47,** 756–762 (2010).
32. Healy, S. J., Gorman, A. M., Mousavi-Shafaei, P., Gupta, S. & Samali, A. Targeting the endoplasmic reticulum-stress response as an anticancer strategy. *Eur. J. Pharmacol.* **625,** 234–246 (2009).

METHODS

Mice. C57BL6/J wild-type mice and *Trif*$^{-/-}$ mice (stock no. 005037) were purchased from the Jackson Laboratory.

Cell culture. Peritoneal macrophages were collected and cultured as previously described[3,33]. MEFs were prepared and cultured as described previously[34].

siRNA, peptides, plasmids and adenoviral constructs. The C(α) subunit of PP2A and eIF2Bε were silenced using siRNA purchased from Qiagen (target sequence for PP2Ac, 5′-CAGGCTGCTATCATGGAATTA-3′; for eIF2B, 5′-ACGGAAGTTG CAACTACAGTA-3′). The coding sequences of wild-type and S535A-mutated rat eIF2Bε (ref. 35) were subcloned into the pcDNA3.1 expression plasmid as described previously[36]. Src activator peptide (Santa Cruz Biotechnology, sc-3052) was delivered to cells using a DirectX peptide transfection kit (Panomics). A plasmid encoding K296R-Y528F-mutated (dominant-negative) Src was purchased from Millipore. An adenoviral vector encoding kinase-inactive Src was a gift from B. Berk (University of Rochester, USA). The plasmids encoding wild-type and L199P-mutated (dominant-negative) PP2Ac were provided by B. Hemmings (Friedrich Miescher-Institut, Switzerland), and the plasmids encoding Y307F-mutated (constitutively active) PP2Ac were provided by D. L. Brautigan (University of Virginia, USA). The coding sequences of human wild-type eIF2Bε, S540A-S544A-mutated human eIF2Bε and S540D-S544D-mutated human eIF2Bε were prepared by Genewiz. In brief, eIF2Bε complementary DNAs (wild-type and mutant, GenBank: NM_003907) were amplified and a FLAG tag was inserted at the 5′ end. The vector was then subcloned into pcDNA3.1(+). A CHOP–GFP reporter plasmid was provided by D. Ron (University of Cambridge, UK). This plasmid was constructed by fusing an 8.5-kilobase 5′ murine CHOP gene fragment to enhanced GFP (ref. 37).

Immunoprecipitation. Cells were lysed with a buffer containing 50 mM HEPES, 150 mM NaCl, 10 mM Na pyrophosphate, 10 mM EDTA, 10 mM EGTA, 1 mM Na orthovanadate, 50 mM NaF, 1 mM phenylmethyl sulphonyl fluoride, 5 μg ml^{-1} leupeptin and 1% Triton-X. The cells or culture media were immunoprecipitated with anti-eIF2Bε (sc-55558) or anti-TNFα (sc-52746) antibody using an ImmunoCruz IP–WB Optima E System (Santa Cruz).

[^{35}S]methionine-cysteine incorporation into global proteins and TNFα. Global protein synthesis was analysed as previously described[3]. For TNFα, the cells were labelled as described in the legend of Fig. 5 and Supplementary Fig. S4. Medium and cells were immunoprecipitated using anti-TNFα, which recognizes both the pro-form (which has a relative molecular mass of 25,000, M_r25K) and the cleaved-secreted form (M_r17K). Approximately equal immunoprecipitated TNFα protein loads per lane were subjected to electrophoresis, and then transferred to a nitrocellulose membrane and immunoblotted for TNFα. For the medium experiment, the membrane was exposed to X-ray film for autoradiography, and the TNFα band was quantified by densitometry. For the cell experiment, the pro-TNFα bands on the immunoblot were cut out and their [^{35}S] c.p.m. was counted by liquid scintillation chromatography.

Immunoblot analysis. Immunoblots were conducted as described previously[38]. All antibodies were purchased from Santa Cruz Biotechnology, except anti-p$^{GSK-site}$-eIF2Bε, anti-p-eIF2α and anti-GFP (Abcam); anti-eIF2α and anti-pTyr416-Src (Cell Signaling Technology); and anti-Flag (Sigma-Aldrich). The dilutions of all primary antibodies were 1:500, except 1:1,000 for p-eIF2α and pTyr416-Src; and 1:3,000 for p-eIF2Bε.

Real-time quantitative PCR. Total RNA from cells was isolated and was reverse-transcribed into cDNA as previously described[3]. Real-time quantitative PCR for *Eif2be* at the phospho-site region and amino-terminal region was conducted using Taqman PCR reagent (Applied Biosystems). For the *Eif2be* phospho-site region, the forward and reverse primers were 5′-GATGAG GAGCTACGGCAGAG-3′ and 5′-CAGGACCTCGTTCTGGAAAA-3′, respectively; the FAM-labelled probe was 5′-TGGACAGCCGAGCAGGCT-3′. For the *Eif2be* N-terminal region, the forward and reverse primers were 5′-ATCTACCGAGGG CCTGAAGT-3′ and 5′-TTTGACTCGCTCCTTGACCT-3′, respectively. Cyclophilin A was used as an internal control[3]. Real-time quantitative PCR for *Tnfa* was conducted using SYBR green reagent (Qiagen). The forward and reverse primers were 5′-CCAGACCCTCACACTCAG A-3′ and 5′-CACTTG GTGGTTTGCTACGAC-3′, respectively.

TNFα ELISA. The level of TNFα in the culture medium was measured by an enzyme-linked immunosorbent assay kit (Thermo Scientific).

eIF2Bε GEF activity assay. GEF activity was assayed as previously described[39] with a modification described in refs 40,41. This assay uses a binary complex of eIF2–[^{3}H]GDP, which was formed by incubating 1.3 μM [^{3}H]GDP (10.7 Ci mmol^{-1}) and rat liver eIF2 for 10 min at 30 °C in a mixture containing 50 mM MOPS, at pH 7.4, 100 mM KCl, 1 mM dithiothreitol, 200 μg ml^{-1} BSA and 2 mM Mg acetate. The reaction mixtures contained 175-μl of cell supernatant fraction in 140 μl of buffer D (50 mM MOPS, at pH 7.4, 209 μM GDP, 2 mM Mg acetate, 100 mM KCl, 1 mM dithiothreitol and 200 μg ml^{-1} BSA) and 87.5 μl of water. The reaction was initiated by adding 35 μl (1–2 pmol) of eIF2–[^{3}H]GDP binary complex (above) to the reaction mixture at 30 °C. After various reaction times, 75-μl aliquots were removed and placed in tubes containing 2.5 ml of ice-cold wash buffer (buffer D without BSA). The contents were mixed and immediately filtered through a nitrocellulose filter disc. The filters were dissolved in 7 ml of Filtron-X, and radioactivity was measured in a liquid scintillation counter.

Preparation of ^{32}P-labelled eIF2Bε. Recombinant eIF2Bε (∼20 μg) was first 'primed' by incubation at 30 °C for 30 min with 13.75 μg GST–DYRK2 (provided by C. Proud, University of Southampton, UK) in a buffer containing 5 mM Tris at pH 7.5, 0.1 mM EGTA, 10 mM Mg acetate and 100 μM ATP. The solution was then passed through a Zeba desalting spin column, and GST–DYRK2 in the flow-through was removed using EZview red glutathione affinity gel beads (Sigma-Aldrich). The remaining primed eIF2B was incubated at 30 °C for 30 min with 100 μCi [γ-^{32}P]ATP and 100 μg His–GSK3β (EMD Chemicals) in a buffer containing 50 mM Tris at pH 7.0, 200 μM ATP, 120 nM microcystin LR, 0.1%(v/v) β-mercaptoethanol, 10% glycerol, 0.1 mM phenylmethyl sulphonyl fluoride, 1 mM benzamidine and 0.01% Brji35. His–GSK3β was then removed by incubating the solution with EZview red His-select HC nickel affinity gel beads (Sigma-Aldrich). The remaining reaction reagents were removed by filtration using a desalting column. To confirm the radiolabelling of eIF2Bε, a small aliquot of the substrate solution was subjected to electrophoresis followed by autoradiography.

Dephosphorylation assay. Cells were lysed in a buffer containing 50 mM Tris at pH 7.4, 1 mM dithiothreitol, 100 μM EDTA, 100 μM EGTA and 0.1% NP-40. Aliquots of lysate (50–80 μg protein) were incubated with 10 μl ^{32}P-labelled eIF2Bε in a buffer containing 50 mM Tris at pH 7.4 and 100 μM $CaCl_2$ (total volume = 130 μl). At 7-min intervals, 10-μl aliquots of the reaction mixture were spotted onto P-81 filter paper discs, which were then washed four times with 0.4% (v/v) phosphoric acid, rinsed once with 100% ethanol and air-dried for liquid scintillation counting.

Metabolic labelling and detection of dephosphorylation of eIF2Bε. Macrophages were treated with LPS for 6 h, and the medium was removed and saved. The cells were then incubated in phosphate-free DMEM supplemented with LPS and 10% dialysed fetal bovine serum for 1 h, followed by addition of [^{32}P]orthophosphate to a final concentration of 0.1 mCi ml^{-1}. After 4 h, the medium was removed and incubated for 14 h in the medium collected from the first 6-h incubation. The cell extracts were subjected to immunoprecipitation using anti-eIF2Bε antibody. Radiolabelled proteins found in the immunoprecipitate were separated by electrophoresis and transferred to nitrocellulose membrane that was exposed to X-ray film for autoradiography and immunoblotted for the input proteins.

Src activity assay. Cells were lysed in the buffer mentioned in the Immunoprecipitation section, followed by immunoprecipitation using anti-pp60^{src} antibody (clone GD11; Millipore catalogue # 05-184) for 2 h at 4 °C. Src kinase activity in the immunoprecipitate aliquots was measured using a commercially available kit (Millipore, catalogue #17-131). Src activity was determined as total kinase activity (without SFK inhibitor, PP1) minus non-Src kinase activity (with PP1).

Apoptosis assay in cultured macrophages. Apoptosis was assayed in cultured macrophages as previously described[38]. Representative fields were captured using an Olympus IX70 inverted fluorescent microscope and a DP71 CCD (charge-coupled device) camera. The number of annexin-V-positive cells was counted and expressed as the percentage of total cells.

Immunofluorescent staining. Macrophages were fixed with 4% paraformaldehyde and permeabilized using 0.1% Triton-X. Immunofluorescent staining for p-Src or p-PP2Ac was carried out using anti-p-Src (Santa Cruz, sc-81521; 1:250 dilution) or anti-p-PP2Ac (sc-271903; 1:250 dilution) antibodies, and AlexaFluor594 donkey anti-mouse IgG (Invitrogen; 1:1000 dilution) as the secondary antibody. Sections were counterstained with DAPI (4,6-diamidino-2-phenylindole) and mounted with ProLong Gold anti-fade reagent (Invitrogen).

DOI: 10.1038/ncb2408

Statistics. Statistical differences between experimental groups were analysed using two-tailed Student's *t*-tests or analysis of variance for experiments with more than two experimental groups.

33. Cook, A. D., Braine, E. L. & Hamilton, J. A. The phenotype of inflammatory macrophages is stimulus dependent: implications for the nature of the inflammatory response. *J. Immunol.* **171,** 4816–4823 (2003).
34. Zinszner, H. *et al.* CHOP is implicated in programmed cell death in response to impaired function of the endoplasmic reticulum. *Genes Dev.* **12,** 982–995 (1998).
35. Jefferson, L. S., Fabian, J. R. & Kimball, S. R. Glycogen synthase kinase-3 is the predominant insulin-regulated eukaryotic initiation factor 2B kinase in skeletal muscle. *Int. J. Biochem. Cell Biol.* **31,** 191–200 (1999).
36. Tuckow, A. P., Vary, T. C., Kimball, S. R. & Jefferson, L. S. Ectopic expression of eIF2Bϵ in rat skeletal muscle rescues the sepsis-induced reduction in guanine nucleotide exchange activity and protein synthesis. *Am. J. Physiol. Endocrinol. Metab.* **299,** E241–E248 (2010).
37. Novoa, I., Zeng, H., Harding, H. P. & Ron, D. Feedback inhibition of the unfolded protein response by GADD34-mediated dephosphorylation of eIF2α. *J. Cell Biol.* **153,** 1011–1022 (2001).
38. Feng, B. *et al.* The endoplasmic reticulum is the site of cholesterol-induced cytotoxicity in macrophages. *Nat. Cell Biol.* **5,** 781–792 (2003).
39. Kimball, S. R., Everson, W. V., Flaim, K. E. & Jefferson, L. S. Initiation of protein synthesis in a cell-free system prepared from rat hepatocytes. *Am. J. Physiol.* **256,** C28–C34 (1989).
40. Rowlands, A. G., Montine, K. S., Henshaw, E. C. & Panniers, R. Physiological stresses inhibit guanine-nucleotide-exchange factor in Ehrlich cells. *Eur. J. Biochem.* **175,** 93–99 (1988).
41. Matts, R. L. & London, I. M. The regulation of initiation of protein synthesis by phosphorylation of eIF-2(α) and the role of reversing factor in the recycling of eIF-2. *J. Biol. Chem.* **259,** 6708–6711 (1984).

DOI: 10.1038/ncb2408

nature cell biology

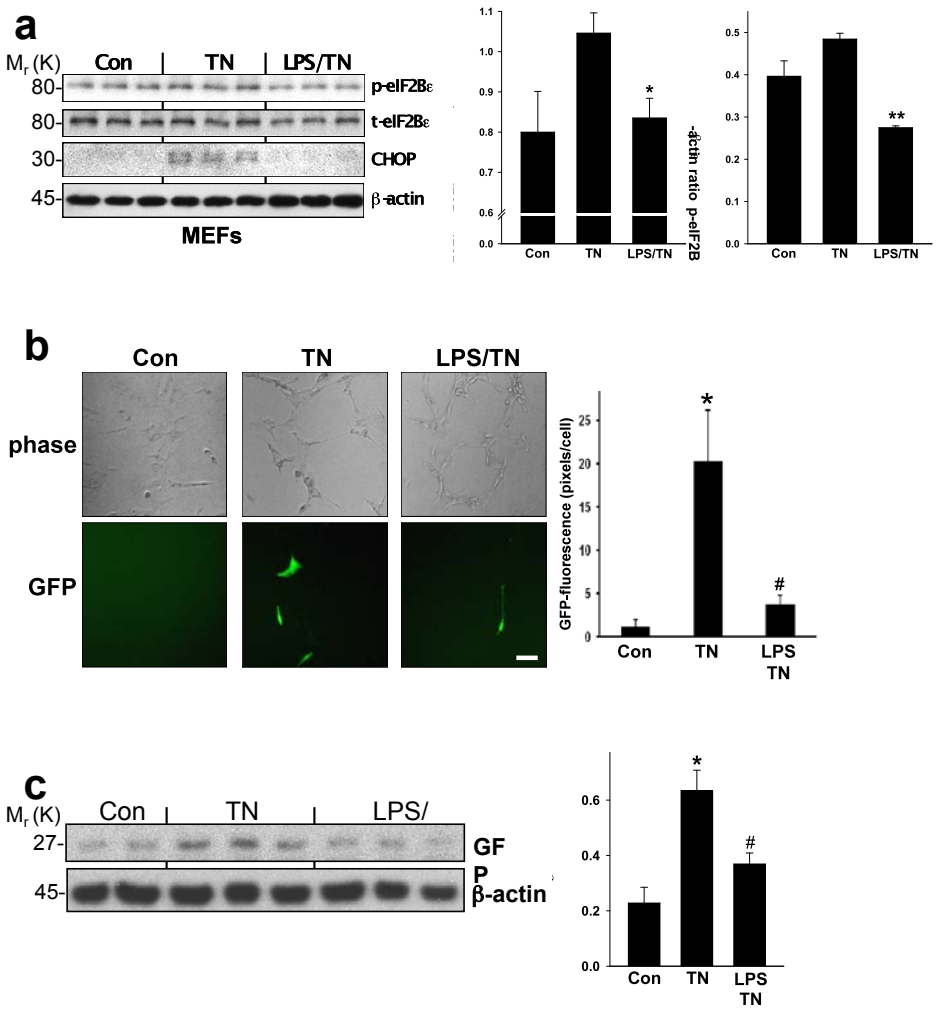

Figure S1 LPS decreases phospho-eIF2Bε and *Chop* promoter-driven reporter expression in ER-stressed MEFs. (**a**) Extracts of control MEFs or MEFs pretreated for 8 h ± LPS (500 ng ml^{-1}) followed by 2-h treatment with tunicamycin (TN, 0.5 μg ml^{-1}) were analyzed by immunoblot for phospho (p)- and total (t) eIF2Bε and b-actin and then quantified by densitometry. *P = 0.04 and **P = 0.002 *vs.* TN. (**b-c**) MEFs were transfected with a *Chop* promoter:GFP construct, and 12 h later, the cells were left untreated (Con) or treated with LPS (500 ng ml^{-1}) for 8 h and then with tunicamycin for 16 h. (**b**) One set of cells was visualized by phase and fluorescence microscopy and quantified for GFP fluorescence intensity. Bar, 100 μm *P < 0.01 vs. control; $^{\#}$P < 0.02 vs. TN. (**c**) Extracts from a parallel set of cells was subjected to immunoblot analysis for GFP and b-actin and quantified by densitometry. *P < 0.02 vs. control; $^{\#}$P < 0.05 vs. TN. Data are expressed as mean ± s.e.m. with n = 3.

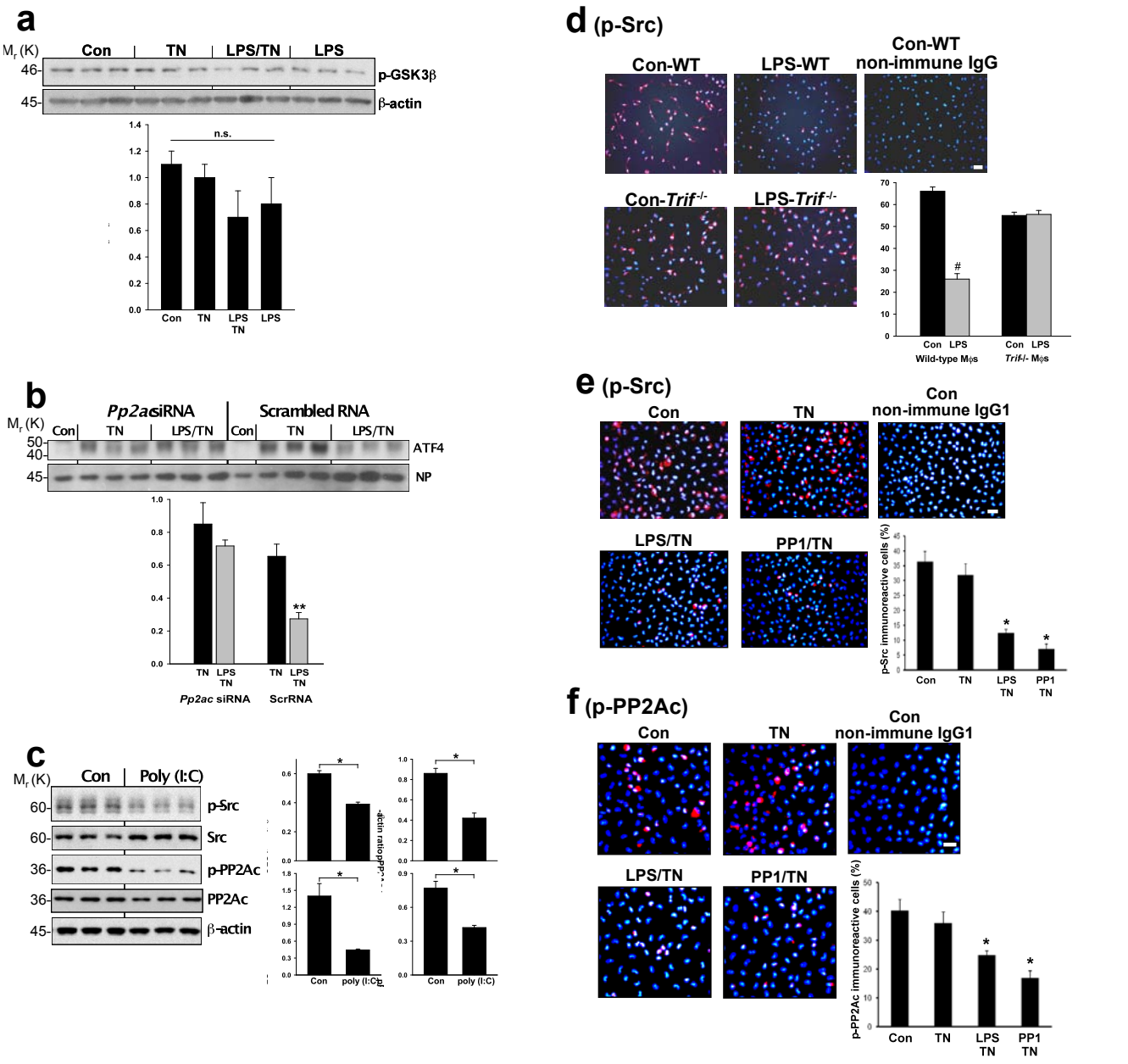

Figure S2 Supplemental data related to the roles of PP2A and SFKs in the TLR-TRIF pathway. In a-b and d-f, macrophages were untreated or pretreated ± LPS (1 ng ml^{-1}) for 24 h. In a, b, e, and f, the cells were then incubated with tunicamycin (TN, 1 μg ml^{-1}) for 3 h, and, in panels e-f, some of the tunicamycin-treated cells were co-treated with the SFK inhibitor PP1 (10 μM). (**a**) Cell extracts were assayed by immunoblot for p-GSK3β and β-actin, and the data were then quantified by densitometry; none of the values were statistically different from each other (n.s., non-significant). (**b**) Macrophages were transfected with scrambled RNA or *Pp2ac* siRNA, and 48 h later the cells were treated as above. Nuclear extracts were probed for ATF4 and nucleophasmin (NP) loading control by immunoblot and then quantified by densitometry. **P < 0.02 vs. TN in the scrambled RNA groups. (**c**) Macrophages were pretreated ± poly(I:C) (2 μg ml^{-1}) for 24 h. Extracts were analyzed by immunoblot for p- and total Src, p- and total PP2Ac, and b-actin and then quantified by densitometry. *P < 0.005. (**d-f**). The cells were fixed with 4% paraformaldehyde and immunostained with anti-p-Src (red) (**d-e**) or anti-p-PP2Ac (red) (**f**). Nuclei are stained with DAPI (blue). Bar, 20 μm. Quantifications of percent of p-Src- or p-PP2Ac-positive macrophages are shown in the bar graphs. Data are expressed as mean ± s.e.m. with n = 3. #P < 0.001 vs. Con-WT and both *Trif*$^{-/-}$ groups (d); *P < 0.01 vs. the Con and TN group (e-f).

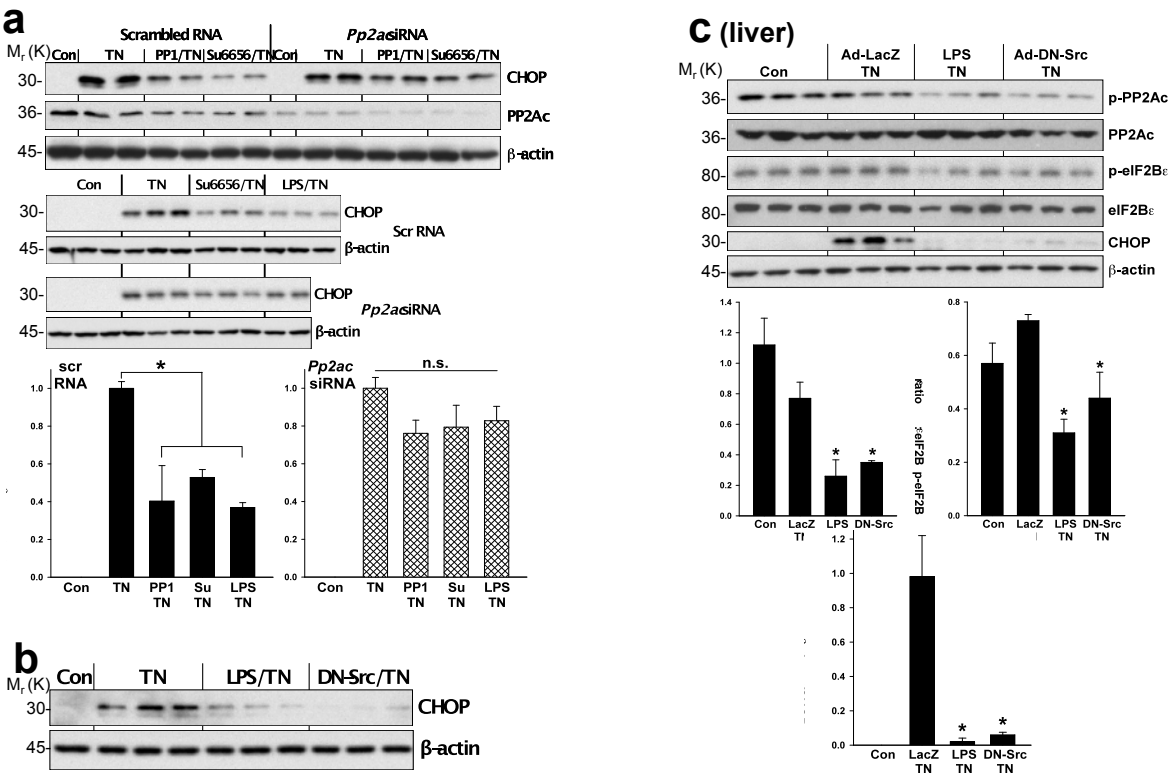

Figure S3 Supplemental data related to the roles of SFKs in the TLR-TRIF pathway. (**a**) Macrophages were transfected with scrambled RNA or *Pp2ac* siRNA. After 48 h, the cells were pretreated for 16 h ± PP1 (5 μM) or Su6656 (20 μM) followed by treatment for 7 h with tunicamycin (TN, 1 μg ml^{-1}). Extracts were analyzed by immunoblot for p- and total PP2Ac, CHOP and b-actin and then quantified by densitometry. *P < 0.05; n.s., non-significant. (**b**) MEFs were pre-incubated for 8 h with LPS (500 ng ml^{-1}) or transfected with a dominant-negative construct of Src (K296R-Y528F; DN-Src). The cells were then incubated under control conditions or treated with tunicamycin (TN, 0.5 μg ml^{-1}) for 2 h. Extracts were analyzed by immunoblot for CHOP and β-actin. (**c**) Mice were injected intravenously with LPS (80 μg kg^{-1}) or vehicle control for 2 consecutive days. On the second day, the mice were injected intravenously with adenovirus expressing either control LacZ (Ad-LacZ) or dominant-negative K296R-Y528F Src (Ad-DN-Src). The mice were then injected with tunicamycin (TN; 1 mg kg^{-1}) intraperitoneally and sacrificed 17 h later. Liver extracts were assayed by immunoblot for p- and total PP2Ac, p- and total eIF2Bε, CHOP, and b-actin. Densitometric quantification of the immunoblot data are shown in the graph and expressed as mean ± s.e.m. with n = 3. *P < 0.05 vs. LacZ-TN.

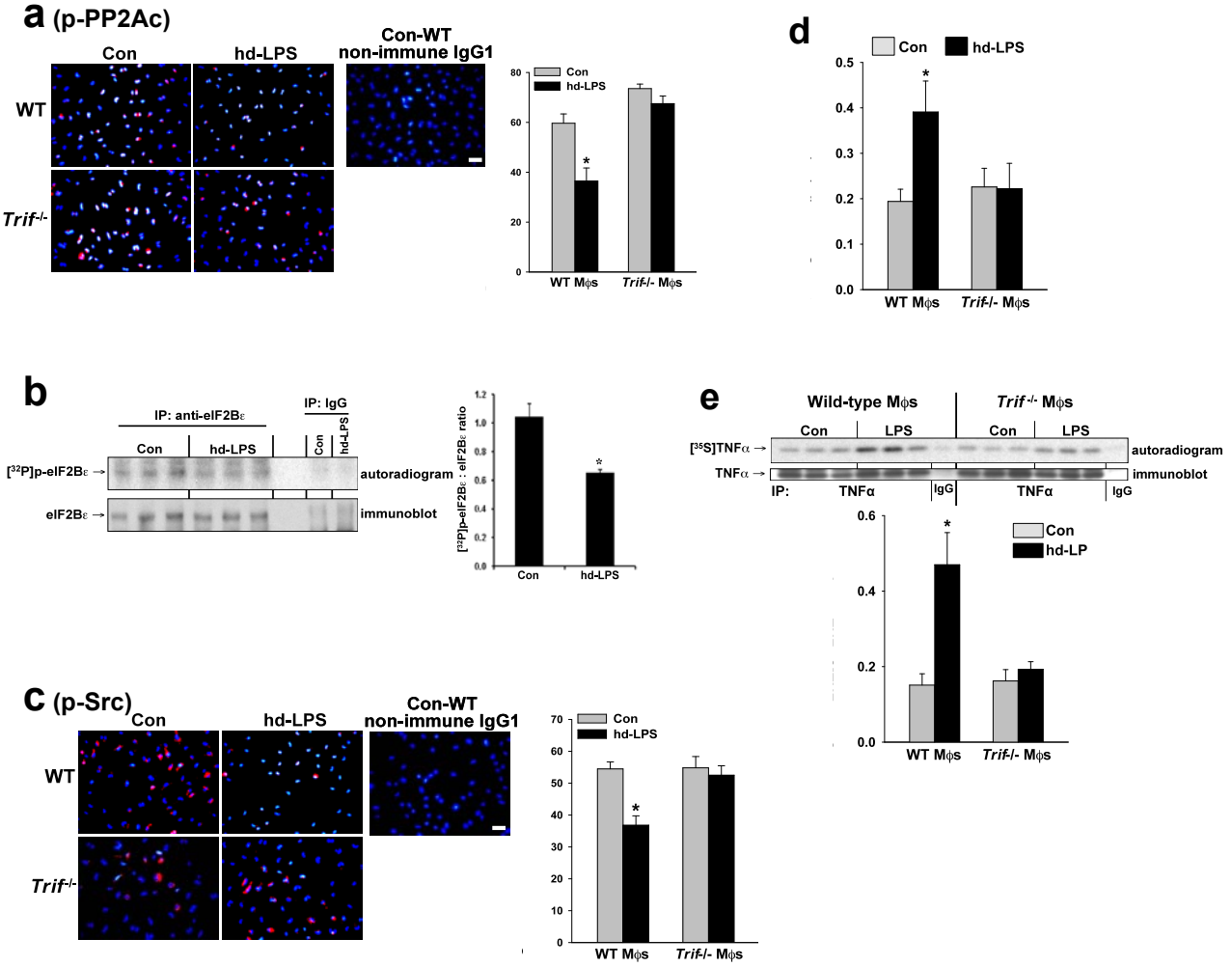

Figure S4 Supplemental data related to the high-dose (hd) LPS model. (**a**) Macrophages were untreated or treated with hd-LPS (1 μg ml^{-1}) for 24 h and then fixed with 4% paraformaldehyde and immunostained with anti-p-PP2Ac (red) and DAPI (blue). Bar, 20 μm. Quantification of percent of p-PP2Ac-positive macrophages is shown in the bar graph. *P < 0.03 vs. WT-con and both *Trif*$^{-/-}$ groups. (**b**) Macrophages were incubated sequentially with hd-LPS for 6 h, followed by phosphate-free medium containing [^{32}P] orthophosphate and hd-LPS for 4 h and then hd-LPS in regular medium again for 14 h. Control cells went through an identical set of incubations but without LPS. Cell extracts were immunoprecipitated for eIF2Bε, followed by SDS-PAGE and transfer to nitrocellulose. The membrane was exposed to X-ray film for autoradiography (top image) and then immunoblotted for eIF2Bε (bottom image). Densitometric quantification of the autoradiogram ([^{32}P] p-eIF2Bε):immunoblot (eIF2Bε, 80 kDa) ratios is shown in the bar graph. *P < 0.04 vs. control. (**c**) Macrophages were untreated or pretreated with hd-LPS for 24 h and then fixed with 4% paraformaldehyde and immunostained with anti-p-Src (red) and DAPI (blue). Bar, 20 μm. Quantification of percent of p-Src-positive cells is shown in the bar graph. *P < 0.03 vs. WT-con and both *Trif*$^{-/-}$ groups. (**d**) Macrophages from wild-type and *Trif*$^{-/-}$ mice were treated for 16 h in the absence (Con) or presence of hd-LPS, and the media were then assayed for TNFα by ELISA. *P < 0.05 vs. the control group. (**e**) Macrophages from wild-type and *Trif*$^{-/-}$ mice were first treated for a total of 16 h in the absence (Con) or presence of hd-LPS, where the last 10 h included [^{35}S]methionine-cysteine in the medium. The media were then immunoprecipitated using anti-TNFα or IgG control, and ~equal amounts of immunoprecipitated TNFα were loaded. After transfer to nitrocellulose, the membrane was exposed to X-ray film for autoradiography (top image) and then immunoblotted for TNFα (bottom image). Densitometric quantification of the autoradiogram:immunoblot TNFα band (17 kDa) ratios is shown in the bar graph. *P < 0.03 vs. WT control and both *Trif*$^{-/-}$ groups. Data are expressed as mean ± s.e.m. with n = 3.

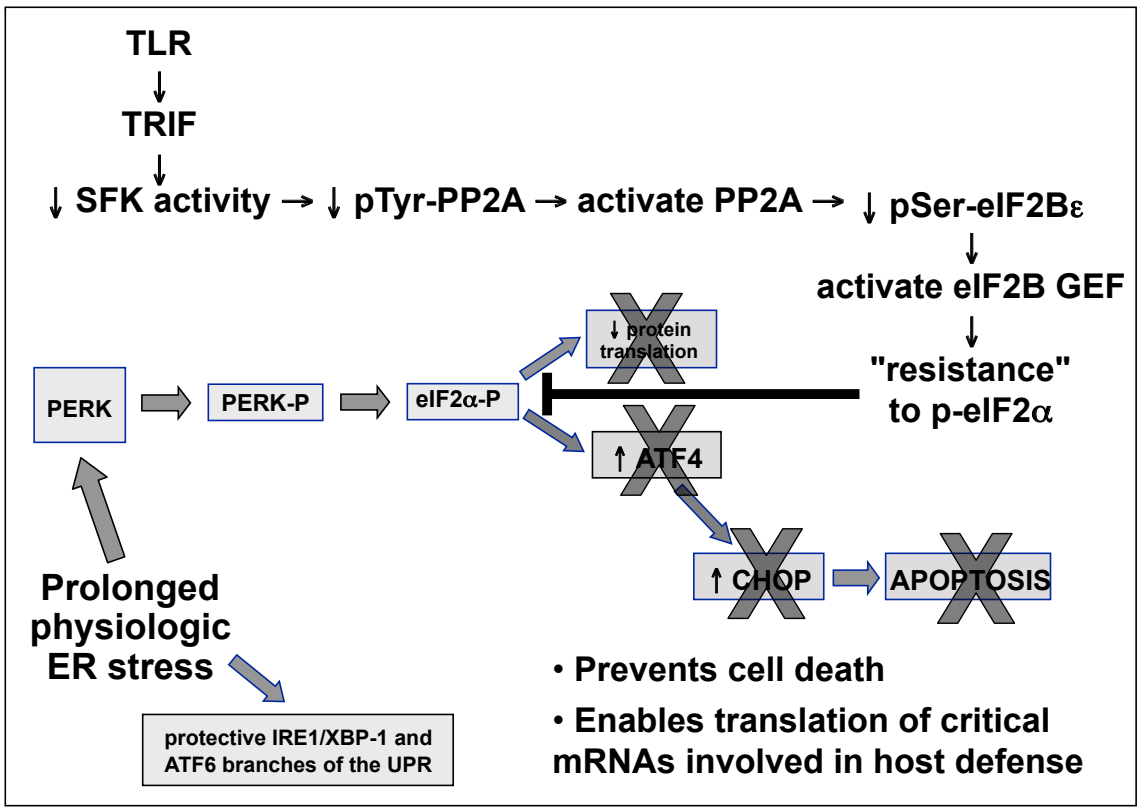

Figure S5 Summary of the pathway through which TLR-TRIF activation enables uninterrupted translation of critical proteins and suppresses cytotoxic CHOP in TLR-TRIF-activated cells, which undergo a prolonged physiologic ER stress response. By activating the GEF activity of eIF2B, the pathway enables uninterrupted global protein translation and suppresses ATF4-CHOP despite phosphorylation of the α-subunit of eIF2 ("p-eIF2a resistance"). The pathway does not affect the other two protective arms of the UPR involving IRE1-XBP-1 and ATF6. We hypothesize that this pathway prevents cell death and enables the translation of critical mRNAs involved in the TLR-induced host defense response, such as *Tnfa*, all in the setting of unperturbed protective UPR signaling. See text for details.

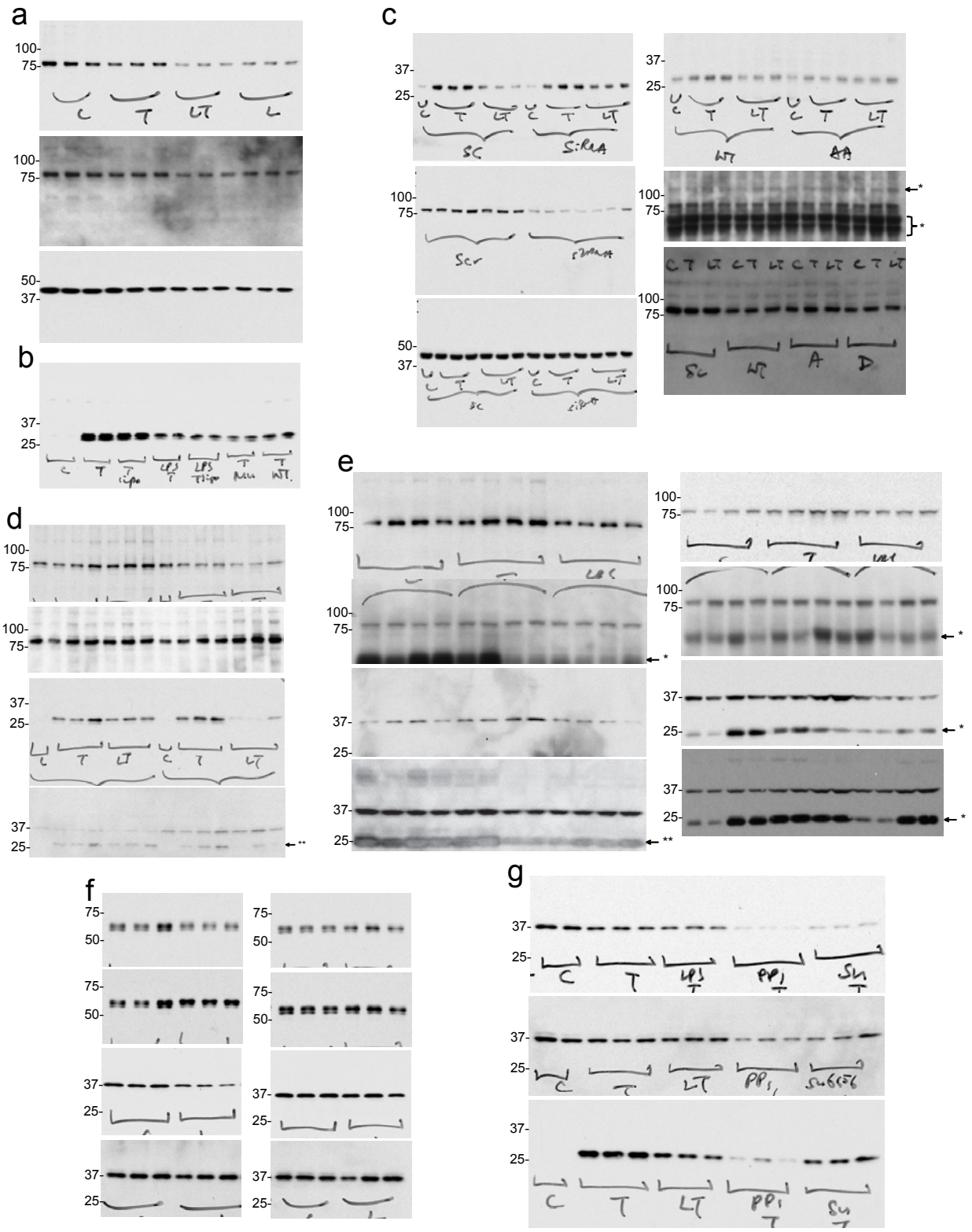

Figure S6 Uncropped western blots shown in the main figures. (**a**) Fig 1c; (**b-c**) Fig 2; (**d-e**) Fig 3; and (**f-g**) Fig 4. The locations of molecular weight markers are on the right side of each blot. *Non-specific bands due to antibody cross-reactivity. **Residual protein bands from a previous immunoblot of the reprobed membrane.

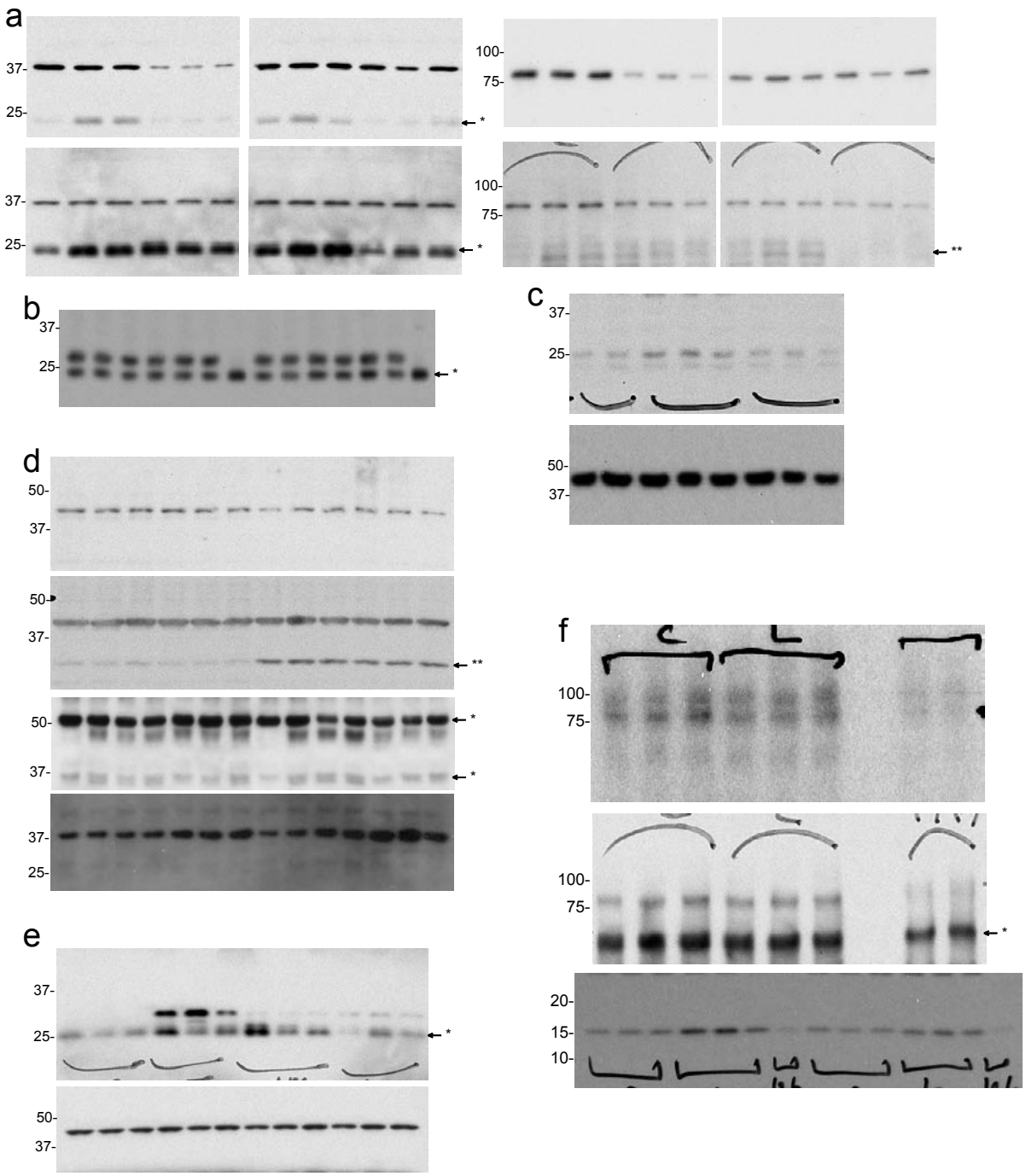

Figure S7 Uncropped western blots shown in the main and supplementary figures. (**a-b**) Fig 5c and 5f; (**c**) Fig S1c; (**d**) Fig S2; (**e**) Fig S3; and (**f**) Fig S4. The locations of molecular weight markers are on the right side of each blot. *Non-specific bands due to antibody cross-reactivity. **Residual protein bands from a previous immunoblot of the reprobed membrane.